Supplementary Manuscript for

A chemical modulator of p53 transactivation that acts as a radioprotective agonist

Akinori Morita*, Ippei Takahashi*, Megumi Sasatani, Shin Aoki, Bing Wang, Shinya Ariyasu, Kaoru Tanaka, Tetsuji Yamaguchi, Akiko Sawa, Yurie Nishi, Tatsuro Teraoka, Shohei Ujita, Yosuke Kawate, Chihiro Yanagawa, Keiji Tanimoto, Atsushi Enomoto, Mitsuru Nenoi, Kenji Kamiya, Yasushi Nagata, Yoshio Hosoi, Toshiya Inaba

*These authors contributed equally to this work.
Corresponding Author: Akinori Morita, E-mail: morita@tokushima-u.ac.jp

This file includes:

Supplementary Methods:

Establishment of a stable p21-knockdown MOLT-4 transformant.

To generate stable transfectants that p21KD-1 cells (a stable p21-knockdown MOLT-4 transformant expressing RNA interference–based p21-targeting shRNAs (Santa Cruz Biotechnology, sc-44214-SH)) and control shRNA-transformant, MOLT-4 cells were transfected with p21-targeting shRNA vectors or a control vector (Santa Cruz Biotechnology, sc-108060) by electroporation (Gene Pulser Xcell, Bio-Rad, 0.25 kV, 950 microfarads), and selected on a 0.16% soft agar culture containing 0.2 μg/ml Puromycin (InvivoGen) for 3 weeks.

5-Chloro-8-methoxyquinoline (5CMQ).

Although 5-chloro-8-methoxyquinoline is a known compound (1), it was synthesized by the different method described below in this work. A solution of 5-chloro-quinolin-8-ol (500 mg, 2.78 mmol), methyl iodide (350 μL, 5.56 mmol) and KOH (312 mg, 5.56 mmol) in THF (8 mL) was stirred at room temperature for 25 h. After concentrating the reaction mixture under reduced pressure, the residue was dissolved in CH_2Cl_2 and washed with water and sat. $NaHCO_3$. The organic layer was dried over Na_2SO_4, filtered, and concentrated under reduced pressure. The obtained residue was recrystallized by hexanes/CH_2Cl_2 to give 5-chloro-8-methoxyquinoline (259 mg, 48% yield) as light brown needles. M.p. 63 °C; ^{1}H NMR (300 MHz, $CDCl_3$/TMS) δ 4.10 (3H, s), 6.98 (1H, d, J = 8.1 Hz), 7.54 (1H, dd, J = 4.8 Hz, 8.4 Hz), 7,57 (1H, t, J = 4.5 Hz), 5.55 (1H, dd, J = 1.8 Hz, 8.4 Hz), 8.95 (1H, dd, J = 1.8 Hz, 4.5 Hz); ^{13}C NMR (75 MHz, $CDCl_3$) δ = 56.1, 76.6, 77.0, 77.4, 107.4, 122.1, 122.4, 126.4, 127.0, 133.0, 149.7, 154.6; IR (neat): 2941, 2839, 1610, 1590, 1566, 1500, 1467, 1439, 1383, 1365, 1306, 1239, 1158, 1127, 1099, 1039, 995, 927, 815, 787, 712, 640, 527 cm^{-1}; HRMS (FAB$^+$); calculated for $C_{10}H_8ClNO$ $(M+H)^+$ 194.0373. found 194.0370.

cDNA sequencing of the *TP53* gene in MOLT-4 cells

Total RNA was extracted from MOLT-4 cells using TRIzol reagent (Invitrogen) according to the manufacturer's instructions. Fist strand cDNA is synthesized with the ReverTra Ace (TOYOBO, Japan) according to the manufacturer's instructions. The *TP53* full-length cDNA containing 5'- and 3'-untranslated region was amplified by PCR using KOD-Plus Neo polymerase (TOYOBO).

The primer sequences were as follows:

(forward) 5'-TGCTTTCCACGACGGTGAC-3'

(reverse) 5'-TCCTCCTCCCCACAACAAAAC-3'.

Thermal cycling was performed in a PCR Thermal Cycler Dice (Takara, Japan) with the following cycling parameters: a 2 min denaturation at 94 °C; followed by 35 cycles of 10 s at 98 °C and 45 sec at 68 °C; except that, in the last cycle, extension was carried out for 3 min. The amplified products (1441 bp) were purified and concentrated by phenol-chloroform extraction and 70% ethanol precipitation, and separated by electrophoresis through a 1.0% agarose gel. The separated products were stained with 1 μg/ml ethidium bromide and visualized under UV light (365 nm), and then picked up from the gel and purified after deep-freezing (at -80 °C) and thawing followed by phenol extraction and 70% ethanol precipitation. The purified DNA was subjected to PCR sequencing using Big Dye Terminator v3.1 cycle sequencing kit (Applied Biosystems) on an automated DNA sequencing system (3130 Genetic Analyzer, Applied Biosystems).

Each sequencing primer sequence was as follows:

(forward-1) 5'-TGCTTTCCACGACGGTGAC-3'

(forward-2) 5'-AACCTACCAGGGCAGCTACG-3'

(forward-3) 5'-AGGTTGGCTCTGACTGTACC-3'

(reverse-1) 5'-CGTAGCTGCCCTGGTAGGTT-3'.

Sequence data were analyzed using CodonCode Aligner V. 6.0.2 software (CodonCode Corporation). Consequently, we confirmed that MOLT-4 cells express Arg72 variant of wt-p53 (codon 72 is CGC), as was confirmed by the demonstration that MOLT-4 cells carry wt-p53 (2-6).

Apoptosis assay

In a flow cytometric analysis, 10,000 cells were analyzed with a flow cytometer (FACS Calibur, Becton Dickinson). Annexin V-FITC staining was performed using a MEBCYTO Apoptosis kit (MBL, Japan) (7). The percentage of cells losing mitochondrial membrane potential ($\Delta\psi m$) and the conformational change of Bax were measured, respectively, by MitoTracker staining and immunofluorescence staining with an anti-Bax monoclonal antibody (mAb) (clone 4F11, MBL), as described previously (7).

Immunoblotting analysis

We used the following antibodies as primary antibodies: caspase-3 (ab90437, abcam), caspase-7 (clone 4G2, MBL, Japan), human p53 (clone DO-1, sc-126 HRP, Santa Cruz Biotechnology), mouse p53 (clone 1C12, Cell Signaling), PUMA (Ab-1, Calbiochem or sc-19187, Santa Cruz Biotechnology), human p21 (clone EA10, Calbiochem), mouse p21 (clone SXM30, BD Pharmingen), β-Actin (clone AC-15, Sigma), pS15-p53 (9284, Cell Signaling), γ-H2AX (JBW301, Millipore), or H2AX (D17A3, Cell Signaling). The protein concentrations of all the protein samples were determined using the BCA Protein Assay Reagent (Thermo Fisher Scientific) and equalized. The band intensities were quantified using ImageJ 1.48v software (National Institutes of Health).

In mouse intestinal analysis, the mouse jejunum was surgically dissected from the intestine with careful removal of the mesentery, washed inside and outside several times with ice-cold physiological saline, and longitudinally shred to open the epithelium. The jejunum was expanded on a piece of flat aluminum foil with the epithelium side up and then aluminum foil was put on an aluminum cube which was kept in a freezer at -80 °C before use. The epithelium was carefully collected by scraping with a surgical blade. In order to avoid cross-reaction between the HRP-conjugated secondary antibodies and mouse blood immunoglobulins, the anti-mouse p53 (clone A-1, sc-393031 HRP, Santa Cruz Biotechnology) and anti-mouse p21 (clone F-5, sc-6246 HRP, Santa Cruz Biotechnology) antibodies were purchased as the HRP-conjugated form, and used for direct detection.

Quantitative PCR (Q-PCR) analysis and Chromatin immunoprecipitation (ChIP) assays

Total RNA was extracted from cells using TRIzol reagent (Invitrogen) according to the manufacturer's instructions. The mouse jejunum was surgically dissected from the intestine with careful removal of the mesentery, cut into pieces, washed inside and outside several times with ice-cold physiological saline, and longitudinally shred to open the epithelium. The epithelium was then carefully washed with ice-cold physiological saline to remove the content of the jejunum, and lysed by flash-soaking the epithelial surface with TRIzol reagent. cDNA synthesis followed by Q-PCR amplification were performed using a Q-PCR reaction mixtures (THUNDERBIRD SYBR qPCR/RT set, TOYOBO) according to the manufacturer's instructions. Q-PCR analysis was performed on an Applied Biosystems 7500 real-time PCR system (Applied Biosystems) as described previously (8, 9).

ChIP assay was performed using EpiQuick ChIP Kit (EPIGENTEK). We used the following antibodies for the immunoprecipitation: normal mouse IgG (EPIGENTEK), Anti- RNA polymerase II (EPIGENTEK), and Anti-p53 (clone DO-1, sc-126, Santa Cruz Biotechnology).

The primers used in these analyses were as follows:

human *CDKN1A*, (forward) 5'-GGTGGCAGTAGAGGCTATGGACA-3'

(reverse) 5'-GGCTCAACGTTAGTGCCAGGA-3'

human *BBC3*, (forward) 5'-AGCCAAACGTGACCACTAGC-3'

(reverse) 5'-GCAGAGCACAGGATTCACAG-3'

human *ACTB* (which encodes β-actin),

(forward) 5'-TGGCACCCAGCACAATGAA-3'

(reverse) 5'-CTAAGTCATAGTCCGCCTAGAAGCA-3'

human *TP53*, (forward) 5'-AGGCCTTGGAACTCAAGGAT-3'

(reverse) 5'-CCCTTTTTGGACTTCAGGTG-3'

human *CDKN1A* for ChIP assay,

(forward) 5'-AGCAGGCTGTGGCTCTGATT-3'

(reverse) 5'-CAAAATAGCCACCAGCCTCTTCT-3'

human *BBC3* for ChIP assay,

(forward) 5'-TTGCGAGACTGTGGCCTTGTGTC-3'

(reverse) 5'-GTCGGACACACACACTGACTGGGA-3'

human *GAPDH* for ChIP assay,

(forward) 5'-TACTAGCGGTTTTACGGGCG-3'

(reverse) 5'-TCGAACAGGAGGAGCAGAGAGCGA-3'

mouse *Cdkn1a*, (forward) 5'-AACATCTCAGGGCCGAAA-3'

(reverse) 5'-TGCGCTTGGAGTGATAGAAA-3'

mouse *Bbc3*, (forward) 5'-GACCTCAACGCGCAGTACGA-3'

(reverse) 5'-GCTCCAGGATCCCTGGGTAA-3'

mouse *Pmaip1* (which encodes Noxa),

(forward) 5'-GGTGGCCAGCAGATACGTGA-3'

(reverse) 5'-GCTTCCAGTAACAGGCAAACCTAGA-3'

mouse *Actb* (which encodes β-actin),

(forward) 5'-CATCCGTAAAGACCTCTATGCCAAC-3'

(reverse) 5'-ATGGAGCCACCGATCCACA-3'

mouse *Lgr5*, (forward) 5'-CTTCACTCGGTGCAGTGCT-3'

(reverse) 5'-CAGCCAGCTACCAAATAGGTG-3'.

Electrophoretic mobility shift assay (EMSA)

Recombinant FLAG-p53 was synthesized and EMSA was performed as described previously (9). The oligonucleotide probe sequences (sense strand) were as follows:

consensus sequence (10), 5'-GGACATGCCCGGGCATGTCC-3'

human *CDKN1A*-based sequence, 5'-TCAGGAACATGTCCCAACATGTTGAGCTC-3'

human *BBC3*-based sequence, 5'- GCGCCTGCAAGTCCTGACTTGTCCGCGG-3'.

Cell cycle analysis

For DNA staining with propidium iodide, 1.5×10^6 cells washed once with PBS were vortex-mixed in 1 ml of 70% ethanol, incubated for 2 h at 4 °C, and washed twice with PBS. The cell pellets were treated with 1 ml of RNase A solution (0.25 mg/ml in PBS) for 30 min at 37 °C followed by adding 100 µl of propidium iodide solution (0.5 mg/ml in PBS) for 30 min at 4 °C. The cells were then analyzed by flow cytometry (FACS Calibur). Cell cycle distribution of diploid cells was analyzed using ModFit LT 3.0 software (Verity Software House).

Hematological parameters in the assessing TBI experiments

In the BM analysis, BM cells were obtained from two femurs and two tibias, and treated with Lysing buffer (BD, Japan) to lyse the red blood cells. BM cells were then counted with an automatic cell counter (ADAM-MC, NanoEnTek, Korea). White blood cell count (WBC), hemoglobin concentration (Hgb), and platelet (PLT) number in peripheral blood were measured by using a hematology analyzer (PCE-310, ERMA). The population of HP stem cells (LSK cells) and progenitor cells in BM cells was measured using flow cytometric analysis as described by Ueda *et al.* (11).

Subtotal-body irradiation (SBI)

Mice, 8 weeks of age, were irradiated with a ^{137}Cs γ-ray source (Gammacell 40 Exactor). Mice were i.p.-injected with vehicle (20% DMSO in olive oil) or with 60 mg/kg 5CHQ 30 min before SBI, and then anesthetized with a pentobarbital sodium 5-10 min before the SBI procedure. Anesthetized mice were placed in the fixation apparatus and irradiated with their front limbs and head shielded, as described in Figure S6. Dosimetry was performed using glass dosimeters in the presence of the lead shields and the fixation apparatus in place. In the presence of the shields, the dose rate was 0.70 Gy/min. All SBI

protocols were reviewed and approved by the Animal Care and Use Committee of Hiroshima University, and were performed in strict accordance with the Guide for the Care and Use of Laboratory Animals by Hiroshima University.

Detection of epithelial proliferation *in situ*

Bromodeoxyuridine (5-bromo-2'-deoxyuridine (BrdU)) incorporation was performed to label the proliferating cells in the small intestine. Mice were intraperitoneally injected with BrdU (50 mg/kg) 30 min before being sacrificed. The specimens were fixed in 10% formalin, embedded in paraffin, and processed routinely for histologic examination. An immunohistochemical study was performed using an anti-BrdU monoclonal antibody (clone B44, BD Biosciences) in accordance with the manufacturer's instructions. A minimum of 50 half crypts was scored per animal.

Intestinal crypt microcolony survival assay

Mice were sacrificed at about 3.5 days after irradiation and the small intestines were removed and fixed with 10% formalin. Intestinal cross sections from paraffin-embedded intestinal bundles were stained with hematoxylin and eosin (H&E) for histological analysis. The total number of cells per crypt section was quantitatively determined by light microscopy, as described in a previous report (12).

Supplementary Figures:

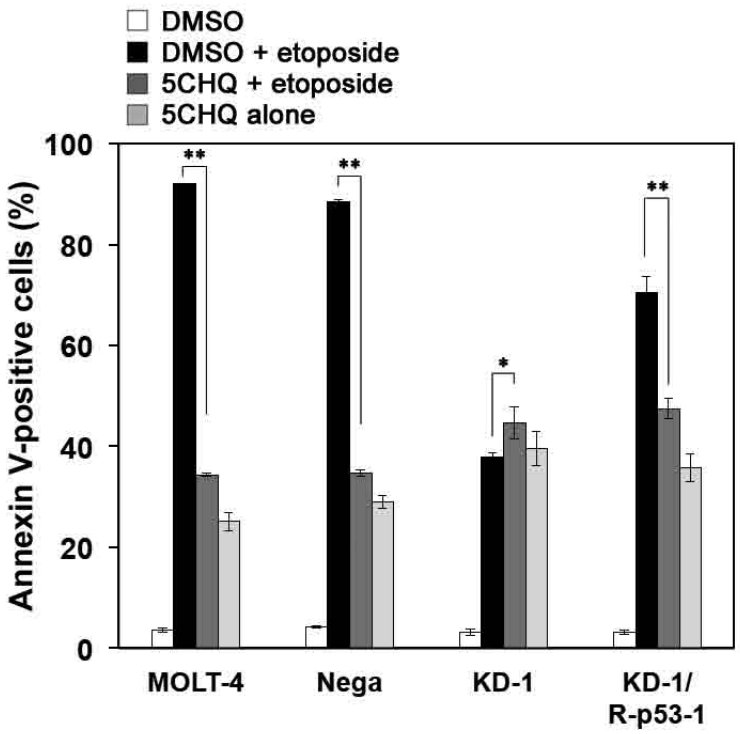

Figure S1. 5CHQ suppresses etoposide-induced apoptosis in wt-p53-expressing cells.

The effect of 40 μM 5CHQ on parental MOLT-4 cells and various MOLT-4 transfectants 17 h after the addition of 5 μM etoposide. Means and standard deviations from three independent experiments are shown and asterisks denote statistical significance: **, $P < 0.01$; *, $P < 0.05$.

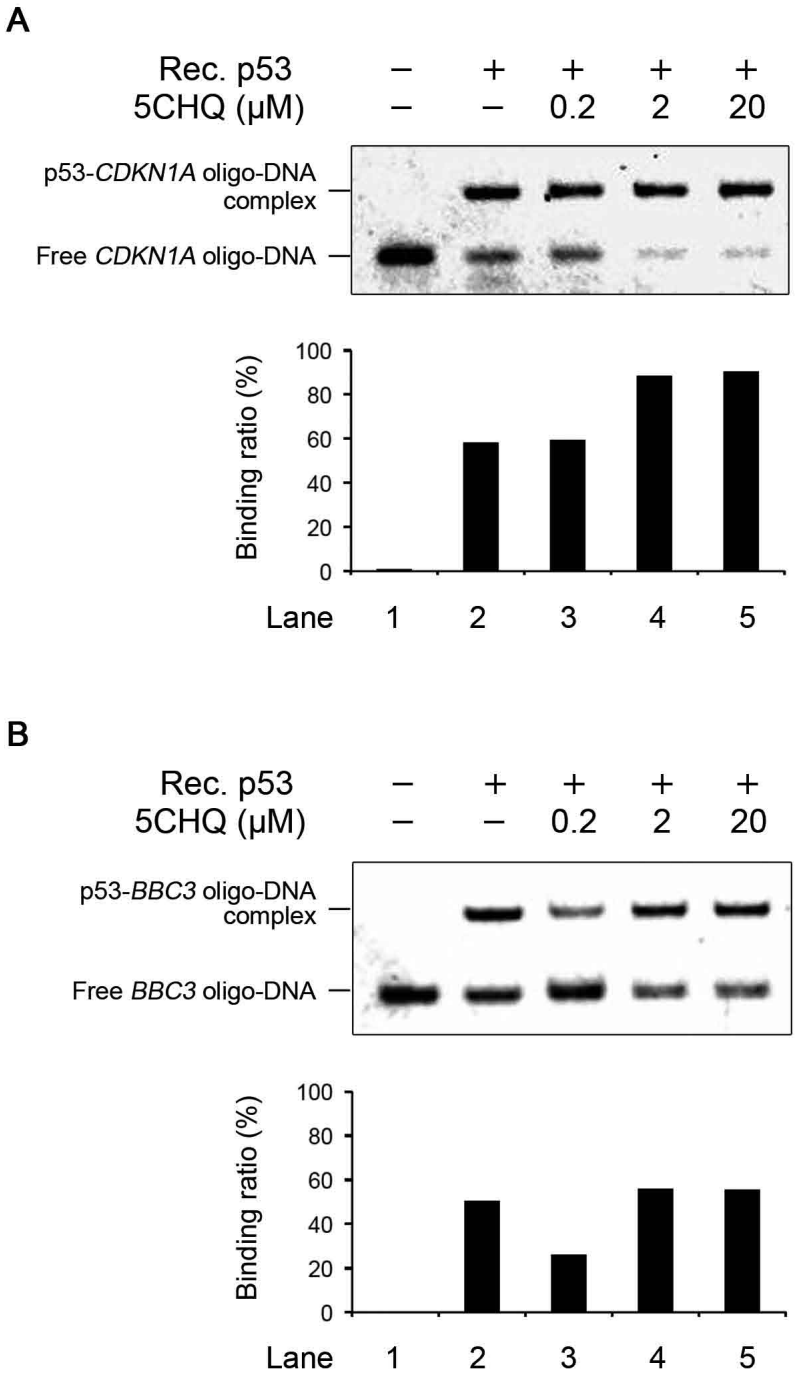

Figure S2. Effect of 5CHQ on p53's DNA-binding to *CDKN1A* and *BBC3* promoter oligonucleotides. A, The affinity of p53's DNA-binding activity to the *CDKN1A* promoter oligonucleotides is upregulated by 5CHQ. B, However, 5CHQ failed to change that to the *BBC3* promoter oligonucleotides. These EMSA data suggest that 5CHQ has a direct action in of promoter sequence-specific alteration in p53.

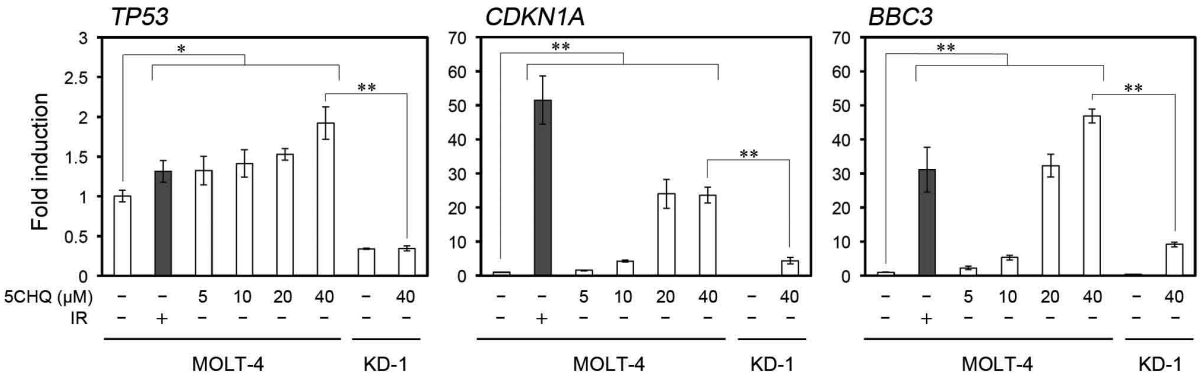

Figure S3. 5CHQ by itself activates p53-mediated transcription.

Q-PCR analysis of *TP53, CDKN1A* and *BBC3* mRNA in MOLT-4 and KD-1 cells. 5CHQ upregulates *TP53, CDKN1A, and BBC3* mRNA transcription at all concentrations tested, even in the absence of irradiation. Means and standard deviations from three independent experiments are shown, and asterisks denote statistical significance: **, $P < 0.01$; *, $P < 0.05$. *P* values of *TP53* analysis are less than 0.05 compared between 5CHQ-treated and vehicle-treated cells. *P* values of *CDKN1A* or *BBC3* analysis are less than 0.01 compared between 5CHQ-treated and vehicle-treated cells. The RNA interference system was leaky to some extent, and could not completely inhibit the expression of *TP53* mRNA in KD-1 cells (66% inhibition). Comparing the mRNA expression between MOLT-4 and MOLT-4-derived knockdown cells at 40 μM of 5CHQ, the inhibition rates by p53 knockdown were 81% (*CDKN1A* mRNA) and 80% (*BBC3* mRNA), respectively. There is no difference for the inhibition rate between the inhibitions of *CDKN1A* mRNA and *BBC3* mRNA by p53 knockdown. Considering that the inhibition rates of two mRNA expressions of p53-target genes (approx. 80%) were higher than that of *TP53* (66%) in the knockdown cells, it is reasonable to consider that these two p53-target genes are predominantly regulated by p53.

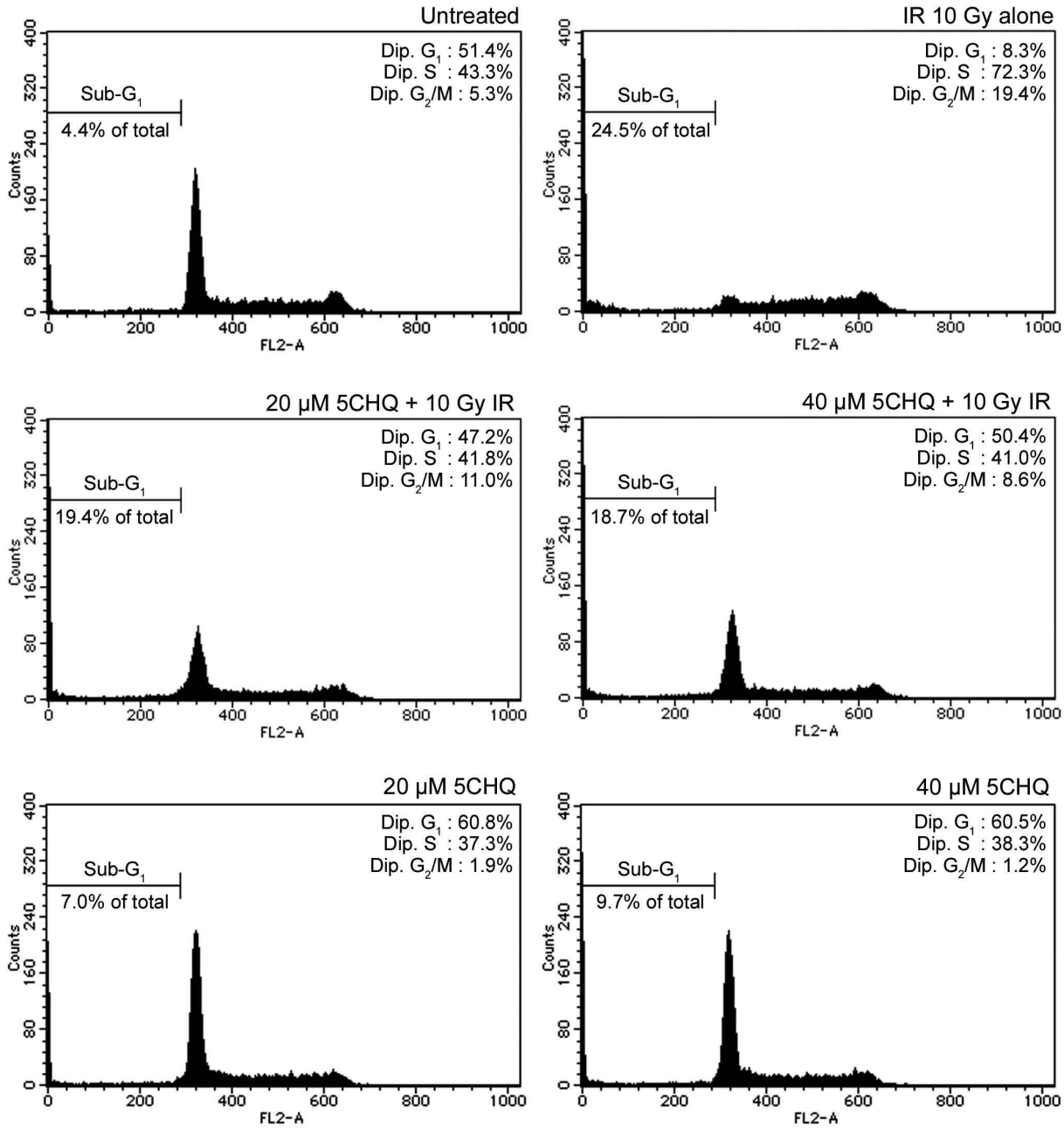

Figure S4. Effect of 5CHQ on cell cycle distribution.

MOLT-4 cells were harvested and treated with RNase A and propidium iodide. The cells were then analyzed by flow cytometry. FL2-A indicates relative the DNA content of propidium iodide fluorescence.

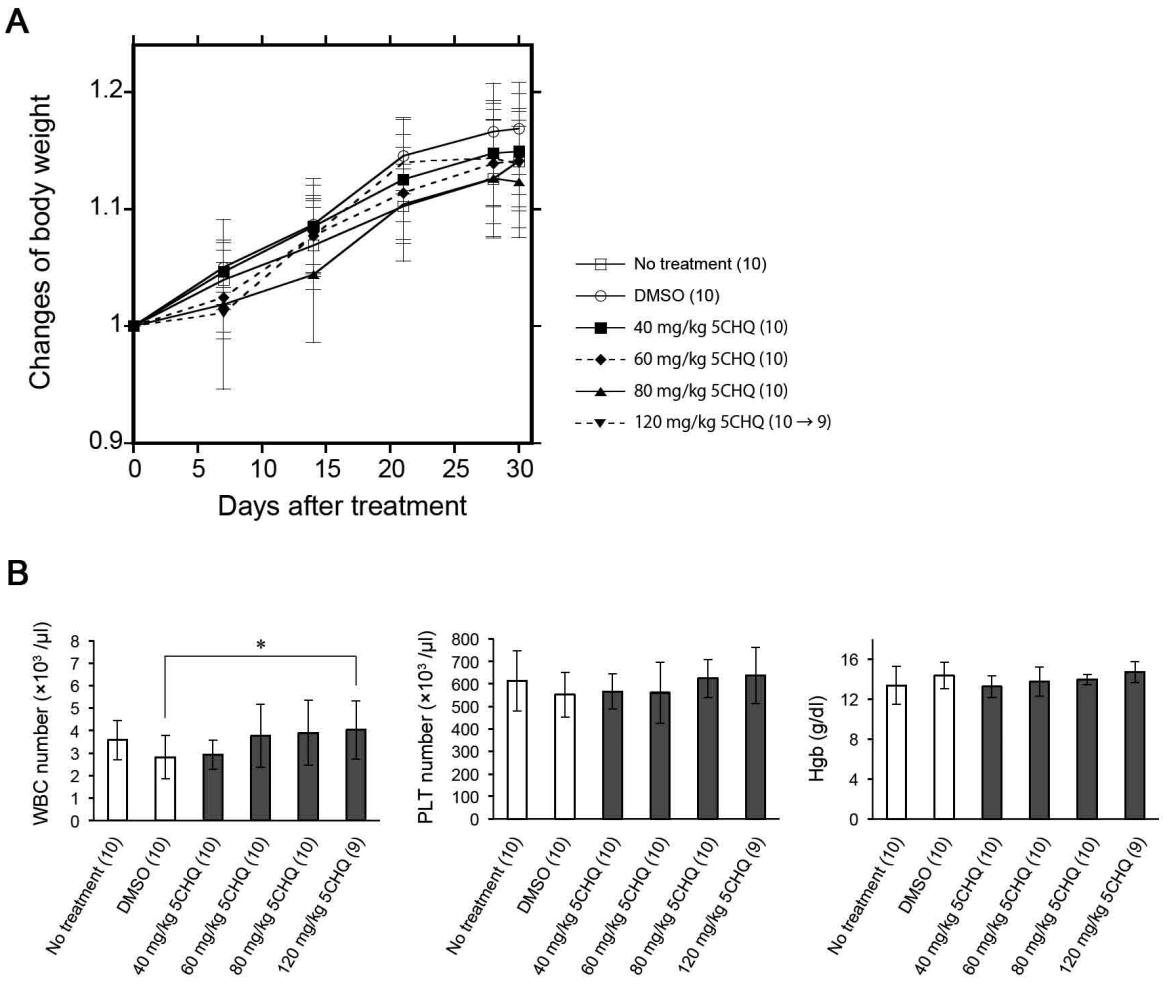

Figure S5. MTD study of 5CHQ.

5CHQ was i.p. administered to ICR mice with vehicle DMSO and olive oil. Numbers before and after arrow in parenthesis denote the number of live mice at start and end, respectively. A, Changes of body weight measured mainly weekly. Only one mouse, which was treated with 120 mg/kg 5CHQ, died in this MTD study. There was no significant difference of body weight among the subgroups of live mice including 9 survived mice treated with 120 mg/kg 5CHQ. B, Change in HP parameters at 31 days of the subgroups of live mice in Figure S5A. There was only a significant difference in the number of WBC between the DMSO-treated and 120 mg/kg 5CHQ-treated subgroups: *, $P < 0.05$.

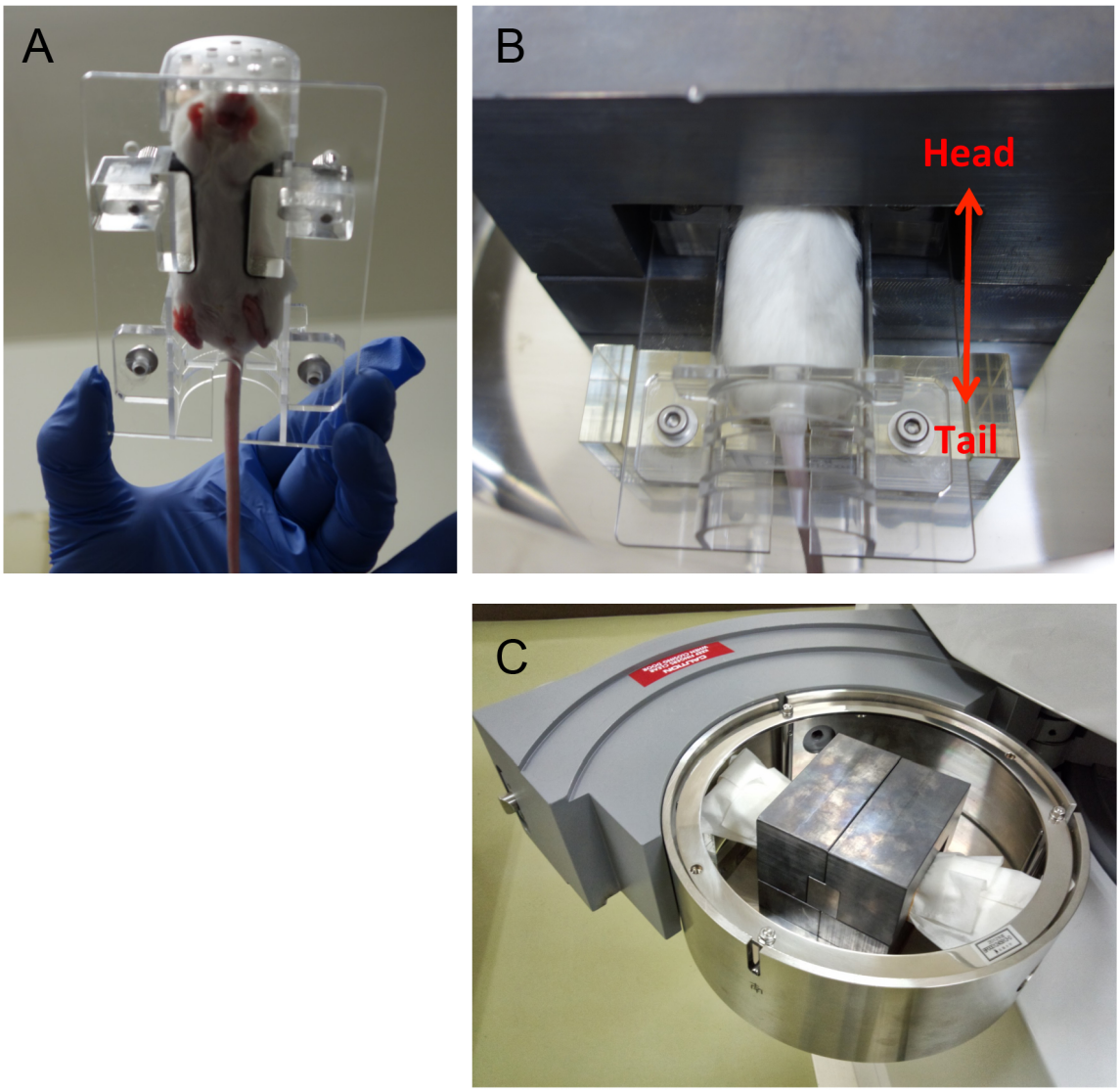

Figure S6. The technique of SBI to avoid BM aplasia.

A, Anaesthetized mice were fixed by clamping the thorax in the fixation apparatus. B, These mice were then irradiated with a γ-ray irradiator (Gammacell 40 Exactor) with head and chest including the BM of the front legs shielded by lead walls at least 3.0 cm thick. C, An entire picture of the SBI apparatus fitting with the γ-ray irradiator. The photograph in the panel B was easily understandable visually, and the actual SBI was performed by wrapping the fixation apparatus, including the mouse, with sterilized filters.

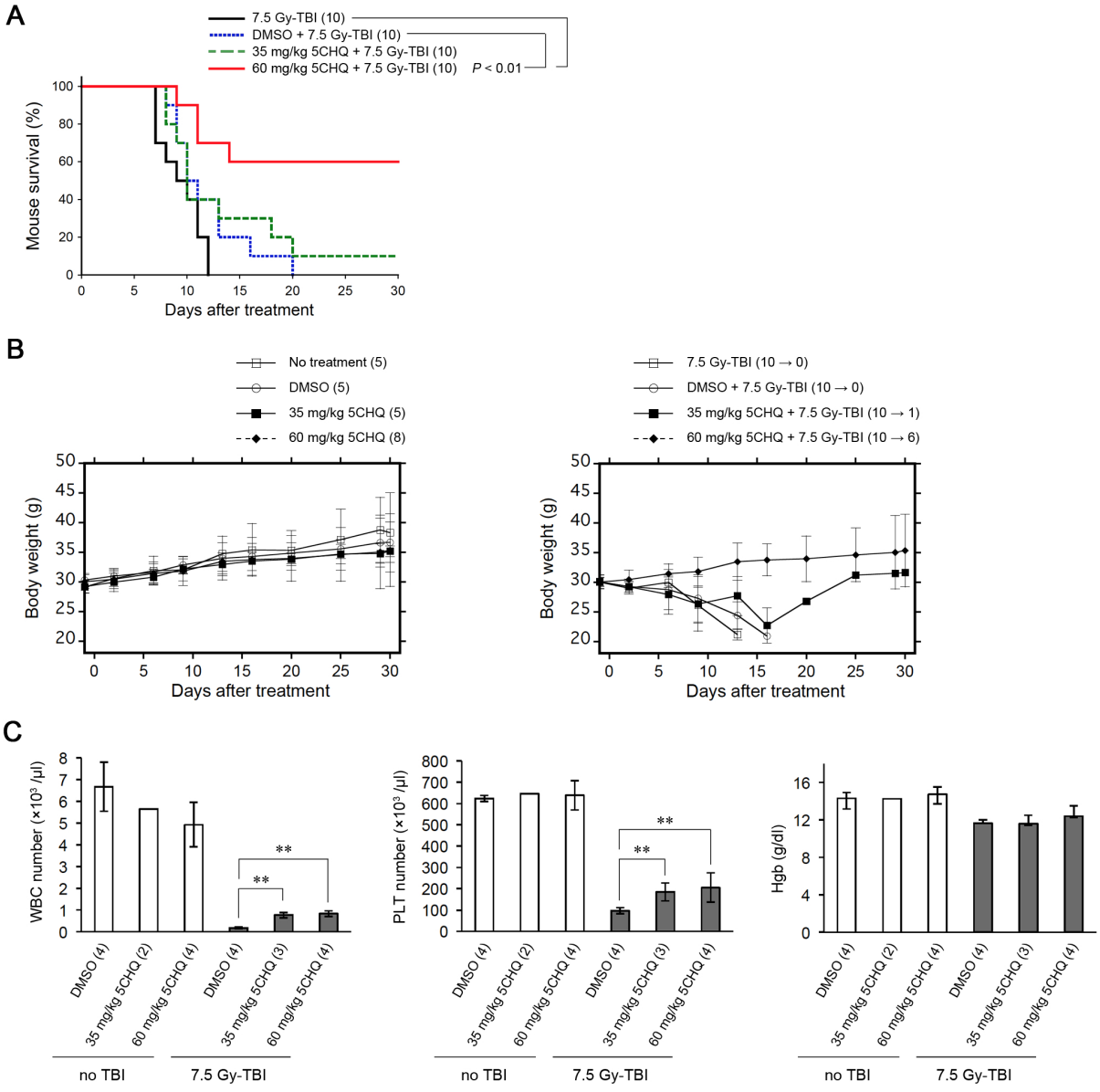

Figure S7. Additional TBI experiments.

ICR mice were i.p. injected with 5CHQ 30 min before 7.5 Gy-TBI. Numbers in parenthesis denote the number of mice. A, Thirty-day survival tests of mouse subgroups of TBI alone, vehicle plus TBI, or 35 mg/kg or 60 mg/kg 5CHQ plus TBI. B, Changes of body weight measured in the experiment of Figure S7A. Numbers before and after arrow in parenthesis denote the number of live mice at start and end, respectively. There was no significant difference of body weight among the mouse subgroups with no TBI (left graph). C, Change in HP parameters at 8 days of mouse subgroups of vehicle plus TBI, or 35 mg/kg or 60 mg/kg 5CHQ plus TBI. There was no significant difference in the number of WBC, PLT, and Hgb between 35 mg/kg and 60 mg/kg 5CHQ plus TBI. Asterisks denote statistical significance: **, $P < 0.01$.

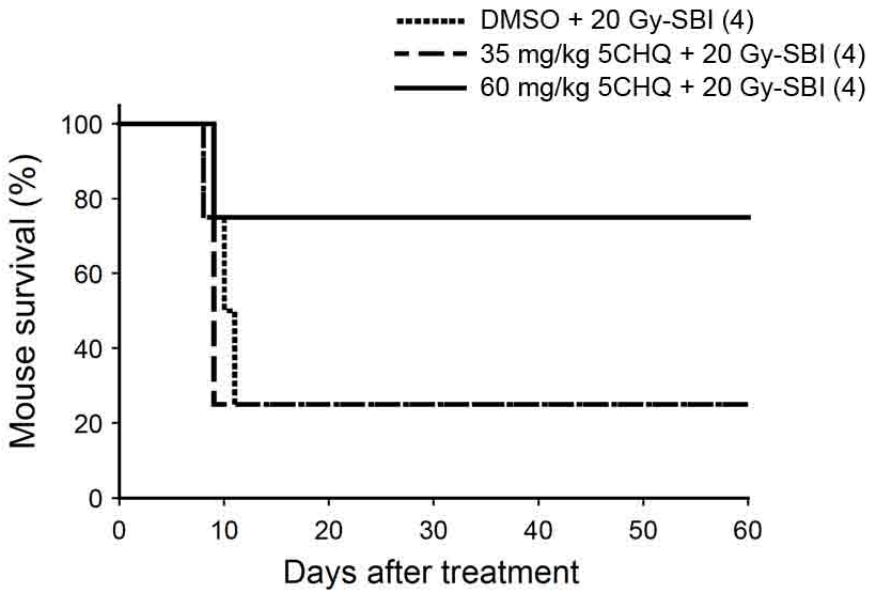

Figure S8. Sixty-day survival test of C57BL/6 mouse after 20 Gy-SBI.

Sixty-day survival tests of mouse subgroups of vehicle DMSO plus SBI, 35 mg/kg or 60 mg/kg 5CHQ plus SBI. Numbers in parenthesis denote the number of mice.

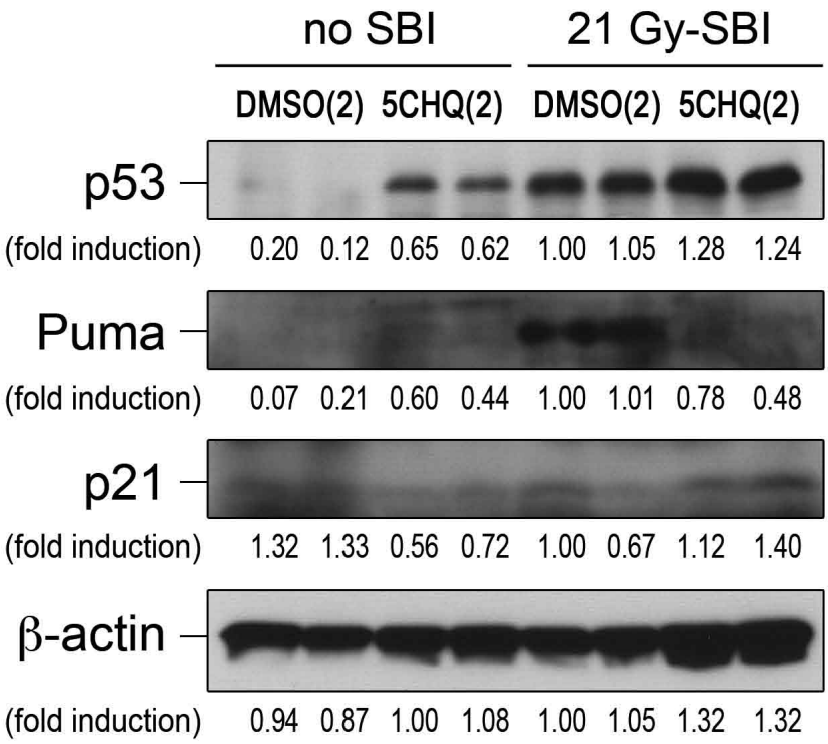

Figure S9. Immunoblotting also revealed the transactivation-modulating activity of 5CHQ.

5CHQ enhanced the induction of mouse p53, p21, and β-actin, but suppressed the induction of Puma 24 h after 21 Gy-SBI in ICR mouse intestinal epithelium. Numbers in parenthesis denote the number of individual mice. Densitometry was performed and the expression level of each band was determined relative to that of the band of the No.1 mouse of the two mice treated with DMSO plus 21 Gy-SBI. Of note, mouse epithelial p53 is also upregulated by 5CHQ alone, indicating the agonistic activity of 5CHQ against p53.

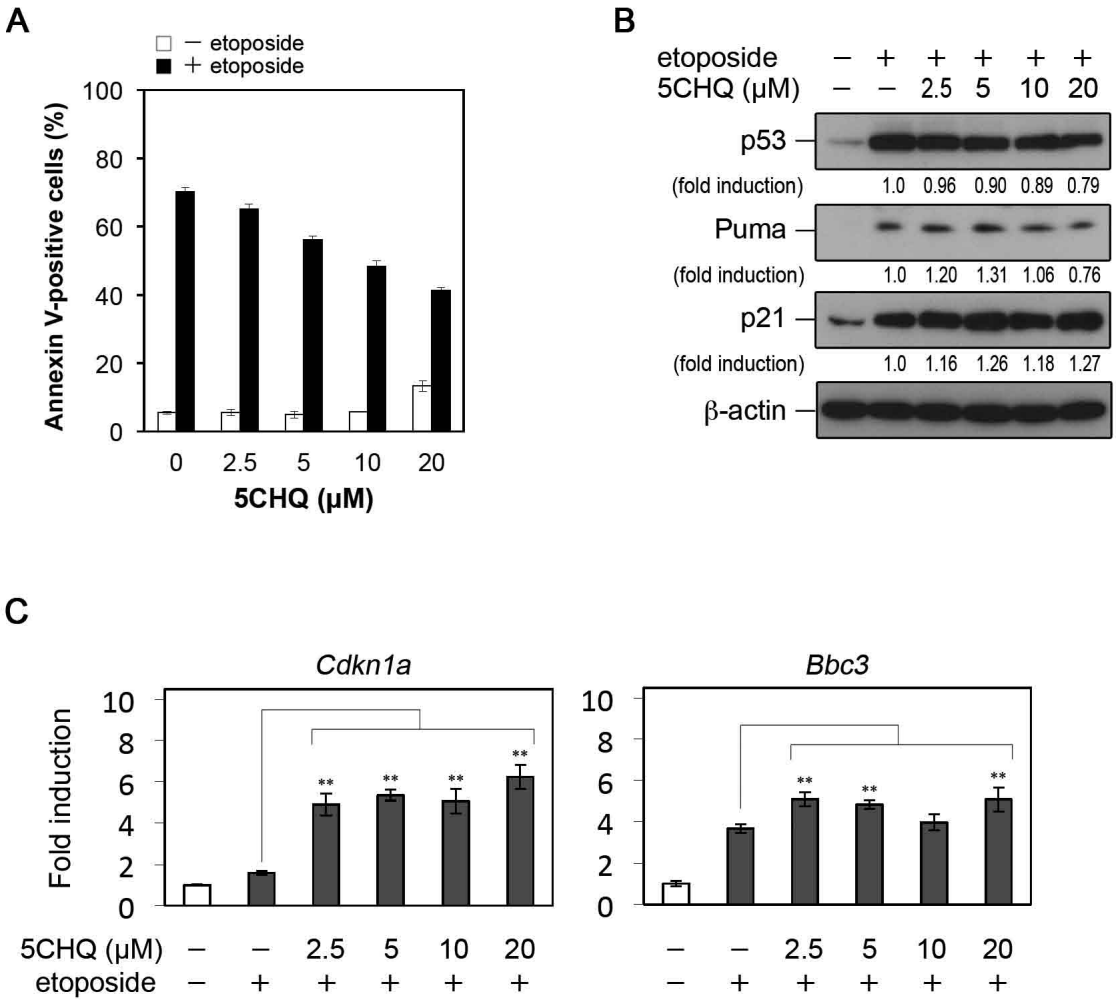

Figure S10. Dose response of 5CHQ on etoposide-induced apoptosis in FM3A cells.

Cells were pretreated with the indicated concentrations of 5CHQ or vehicle (DMSO) for 1h, and then treated with 50 μM etoposide or vehicle. A, Annexin V-FITC staining 20 h after the addition of etoposide. 5CHQ decreased apoptosis at 2.5-20 μM ($p < 0.01$). Means and standard deviations from three independent experiments are shown. B, Immunoblotting detection of p53 and p53 target gene products p21 and Puma 8 h after the addition of etoposide. β-actin was used as an internal control. Band intensities were quantified by densitometry. C, Q-PCR analysis of the transcription of *CDKN1A* and *BBC3* 8 h after the addition of etoposide. Means and standard deviations from 6 independent experiments are shown and asterisks denote statistical significance: **, $P < 0.01$.

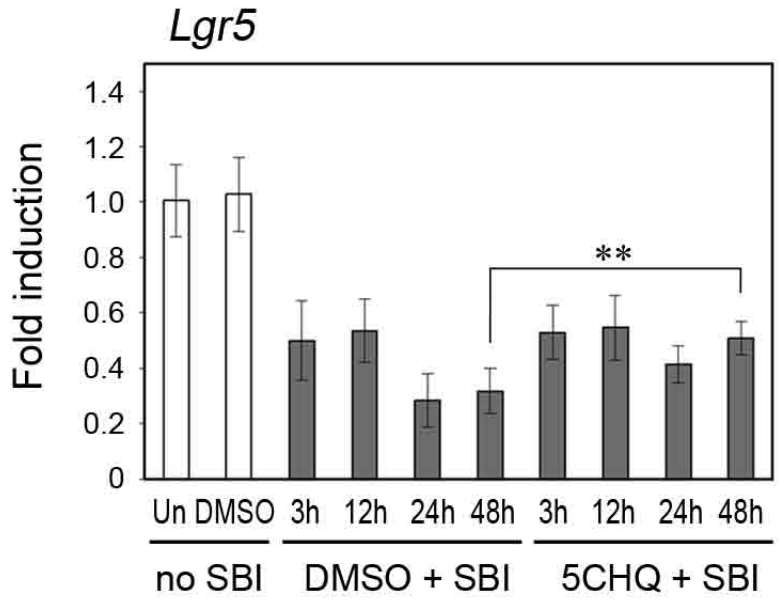

Figure S11. 5CHQ relieves the decrease of the stem cell marker *Lgr5* mRNA expression after SBI.

Q-PCR analysis of the stem cell marker *Lgr5* mRNA expression. 5CHQ enhanced 1.6-fold *Lgr5* mRNA expression compared to DMSO-treated GI epithelium 48 h after 21 Gy-SBI ($P = 0.0091$), and other time points showed no significant difference between 5CHQ-treated and vehicle-treated mice. Means and standard deviations from 4 ICR mice are shown.

References:

1. Weizmann M, Bograchov E. Derivatives of 5-chloro-8-hydroxyquinoline. J Am Chem Soc 1947;69:1222-3.
2. Cheng J, Haas M. Frequent mutations in the p53 tumor suppressor gene in human leukemia T-cell lines. Mol Cell Biol 1990;10:5502-9.
3. Oconnor PM, Jackman J, Bae I, Myers TG, Fan S, Mutoh M, et al. Characterization of the p53 tumor suppressor pathway in cell lines of the National Cancer Institute anticancer drug screen and correlations with the growth-inhibitory potency of 123 anticancer agents. Cancer Res 1997;57:4285-300.
4. Gong BD, Chen Q, Endlich B, Mazumder S, Almasan A. Ionizing radiation-induced, Bax-mediated cell death is dependent on activation of cysteine and serine proteases. Cell Growth Differ 1999;10:491-502.
5. Jia LQ, Osada M, Ishioka C, Gamo M, Ikawa S, Suzuki T, et al. Screening the p53 status of human cell lines using a yeast functional assay. Mol Carcinog 1997;19:243-53.
6. Nakano H, Kohara M, Shinohara K. Evaluation of the relative contribution of p53-mediated pathway in X-ray-induced apoptosis in human leukemic MOLT-4 cells by transfection with a mutant p53 gene at different expression levels. Cell Tissue Res 2001;306:101–6.
7. Morita A, Zhu J, Suzuki N, Enomoto A, Matsumoto Y, Tomita M, et al. Sodium orthovanadate suppresses DNA damage-induced caspase activation and apoptosis by inactivating p53. Cell Death Differ 2006;13:499-511.
8. Wang B, Tanaka K, Morita A, Ninomiya Y, Maruyama K, Fujita K, et al. Sodium orthovanadate (vanadate), a potent mitigator of radiation-induced damage to the hematopoietic system in mice. J Radiat Res 2013;54:620-9.
9. Morita A, Ariyasu S, Ohya S, Takahashi I, Wang B, Tanaka K, et al. Evaluation of Zinc (II) chelators for inhibiting p53-mediated apoptosis. Oncotarget 2013;4:2439-50.

10. Funk WD, Pak DT, Karas RH, Wright WE, Shay JW. A transcriptionally active DNA-binding site for human p53 protein complexes. Mol Cell Biol 1992;12:2866-71.

11. Ueda T, Nagamachi A, Takubo K, Yamasaki N, Matsui H, Kanai A, et al. Fbxl10 overexpression in murine hematopoietic stem cells induces leukemia involving metabolic activation and upregulation of Nsg2. Blood 2015;125:3437-46.

12. Withers HR, Elkind MM. Microcolony survival assay for cells of mouse intestinal mucosa exposed to radiation. Int J Radiat Biol Relat Stud Phys Chem Med 1970;17:261-7.